EVOLUTION OF THE FLOW THROUGH A TURNING MID TURBINE FRAME APPLIED BETWEEN A TRANSONIC HP-TURBINE STAGE AND A COUNTER-ROTATING LP-TURBINE

Cornelia Santner°, Berardo Paradiso°, Franz Malzacher*, Martin Hoeger*,

Josef Hubinka°, Emil Göttlich°

° Institute for Thermal Turbomachinery and Machine Dynamics
Graz University of Technology, Austria
* MTU Aero Engines, Munich, Germany

ABSTRACT

To enhance the performance of modern high-bypass jet engines a promising approach is to replace the low pressure-vane row arranged downstream of a strutted intermediate turbine diffuser (mid turbine frame) by the application of turning struts and to integrate functionalities such as bearing supports, lubrication pipes, engine mounts and aggressive duct designs. Thus the weight may be reduced which results in a lower specific fuel consumption and reduced CO_2-emissions. The additional functions of the mid turbine frame (MTF) structures lead to constraints like a minimum required strut thickness leading to a maximum possible number of struts. Therefore a highly three-dimensional design of the airfoils and the duct, respectively, is necessary to reduce strong secondary flow effects and further to provide suitable flow angle and Mach number for the following low pressure turbine (LPT).

A future area of application for mid turbine frames with turning struts, so-called turning mid turbine frames (TMTF), may also be in direct-drive open-rotor engine architectures. There the LPT with contra-rotating stator and rotor blades is arranged at relatively large radii and the rear bearings of these shafts are supported in the TMTF.

The present paper examines a configuration consisting of a transonic HPT stage followed by an S-shaped TMTF and a counter-rotating LPT rotor at larger diameter. The test arrangement was applied in the newly designed continuously operating two-spool-two-stage turbine rig at Graz University of Technology. To gain a better understanding of the turbulent and unsteady flow field through the MTF which is dominated by strong secondary flows as well as the complex interactions between the components, detailed experimental investigations were performed by means of five-hole-probes at duct inlet and exit as well as downstream the LPT. The results from this unique HPT-Duct-LPT configuration will allow the designers to investigate how to reach optimal designs.

NOMENCLATURE

Symbols

α	[deg]	= $\tan^{-1}(c_t/c_{ax})$ yaw angle positive yaw angle in rotational direction of HPT
γ	[deg]	= $\tan^{-1}(c_r/c_{ax})$ pitch angle
$\Delta H/c_u^2$	[-]	work parameter
C_p	[-]	pressure recovery coefficient
c_{ax}	[m/s]	axial, radial and tang. velocity

h_{inlet}	[mm]	duct height at inlet
H	[mm]	blade height
l	[mm]	duct length
L_{ax}	[mm]	axial duct length
p	[bar]	static pressure
p_n	[bar]	static pressure at position n
p_t	[bar]	total pressure
Re	[-]	=f(chord, c_2) Reynolds number
s	[mm]	tip gap

Abbreviations

3D	three-dimensional	IPT	intermediate pressure turbine
AR	area ratio	LPT	low pressure turbine
CFD	computational fluid dynamics	LPV	lower passage vortex
DREAM	Validation of Radical Engine Architecture Systems	PS	pressure side
		SS	suction side
FHP	five-hole-probe	TMTF	turning mid turbine frame
HPT	high pressure turbine	TTTF	transonic test turbine facility
		UPV	upper passage vortex

INTRODUCTION

To increase efficiency by reducing weight, fuel burn and costs is a very important issue for the development of future jet engines. Another aspect which should not be neglected is to reduce the noise level. These objectives lead to turbofan engines with very high by-pass ratios. Another promising concept is the open-rotor technology investigated in the EU project DREAM. One examined configuration within this project is the jet engine with two counter-rotating open rotors placed at the rear part of the engine. This design requires the engine mount of the rear bearing which is usually positioned downstream the LP turbine to be shifted further upstream between the HPT and LPT. Therefore, the intermediate turbine duct guiding the flow from the HPT to the larger diameter LPT has to be equipped with rigid struts which contain the support of the rear bearings of all shafts and service lines.

This design is also a promising approach for high by-pass ratio turbofan engines in order to reduce the length and the weight of the engine due to an overhung LPT design without turbine end casing and load-carrying LPT casing. A number of publications deal with S-shaped intermediate turbine ducts with non-lifting struts. Norris et al. for example show the performance and flow stability of inter-turbine diffusers with struts. Wallin et al. (2008) and Arroyo Osso et al. (2008) performed experimental and numerical investigations of such a configuration at design and off-design inlet conditions, respectively.

An additional reduction of length and further weight is to integrate the function of the first vane row of the LP turbine in the strutted intermediate turbine duct by introducing turning struts. These wide chord vanes have low aspect ratios (about 0.5) due to the need to be able to provide the LPT with the right inflow conditions. This leads to a highly three-dimensional (3D) flow field dominated by strong secondary flows and 3D boundary layers. These complex flow structures make it inevitable to perform experimental tests to validate CFD simulations but there is a lack of experimental data. Pullan et al. (2003) and Pullan et al. (2005) performed investigations on a low aspect ration vane with a downstream arranged turbine but without a strongly S-shaped duct and no upstream HPT stage. Furthermore, Harvey et al. (2002) examined an intermediate pressure (IP) stage with a low aspect ratio vane applied downstream of a HP stage. There the stage efficiency was increased by introducing non-axisymmetric endwall contouring on the low aspect ratio vane passage and the IPT blade passage. Of course the inclination of such a flow channel representing a three-shaft turbofan is much lower compared to the TMTF setup. Some work was performed at Graz University of Technology where a TMTF or so-called integrated concept was investigated downstream a transonic HPT stage; see Marn et al. (2009a). Furthermore, Miller et al. (2004) investigated the effect of an upstream arranged HPT onto a low aspect-ratio vane. Lavagnoli et al. (2010) investigated a further attempt to unify the exit flow of a TMTF setup by including splitter vanes between the large structural turning struts. But these tests were performed without a downstream arranged LPT like it is the fact in a real engine.

To be able to perform more engine realistic measurements the existing transonic test turbine facility (TTTF) with a single transonic HPT stage was extended with a counter-rotating LP turbine with a larger diameter, see Hubinka et al. (2011). With this modular rig architecture different transition duct and TMTF configurations can be investigated. The adaptation of the rig was performed within the EU project DREAM where one task is to gain a better understanding of the

flow features in a TMTF. Therefore, experimental tests for two different TMTF setups have been performed. The aero design of the rig together with the TMTF baseline design was done by MTU Aero Engines. The second configuration was designed by Volvo Aero. They were tested at the new two-spool transonic test turbine facility at Graz University of Technology. One main objective was that both configurations should provide the similar inflow conditions to the LP rotor. The second setup was designed 10 % shorter with the main objectives to not increase the losses and to provide similar exit flow conditions like the baseline design. The main parameters to match were the flow function (reduced mass flow) and the exit swirl angle of the TMTF. Such an aggressive design would lead to a separation in the strut suction side – hub corner and therefore non-axisymmetric endwall contouring was applied at the TMTF hub contour in order to suppress this.

The present paper shows the first results from the measurements of the basic configuration designed by MTU by means of static pressure taps, five-hole-probes (FHP) as well as oil flow visualization.

EXPERIMENTAL SETUP

To allow realistic investigations of the flow through different turning mid turbine frame configurations the transonic test turbine facility (TTTF) at the Institute for Thermal Turbomachinery and Machine Dynamics has been extended with a counter-rotating low-pressure turbine at larger diameter.

Test Facility

The Transonic Test Turbine Facility (TTTF) is a continuously operating two-stage cold-flow open-circuit plant, which consists of a transonic HPT stage and a counter-rotating LPT stage. This unique configuration allows the testing of rig inserts with a diameter up to 800 mm under engine-representative conditions. Both turbines are designed with overhung-type turbine shafts and additionally the LPT is mounted on an axially moveable frame. This allows easy disk assembly without dismantling the bearings and the simple application of transition duct and TMTF designs with different axial lengths. The facility is driven by pressurized air delivered by a separate 3 MW compressor station in the second basement of the institute. The shaft power of the HPT stage drives a three-stage radial brake compressor. This brake compressor delivers additional air mixed to the flow from the compressor station and increases the overall mass flow. The air temperature at turbine stage inlet can be adjusted by coolers between 40 °C to 185 °C. The maximum shaft speed of the HPT stage is limited to 11550 rpm. Depending on the stage characteristic a maximum coupling power of 2.8 MW at a total mass flow of 22 kg/s can be reached. The power of the LP turbine is absorbed by a waterbrake with a maximum power of 700 kW. Detailed information on the design and construction of the original single stage facility can be found in Erhard and Gehrer (2000), on the operation in Neumayer et al. (2001). For the design of the LP-stage together with the TMTF see Hubinka et al. (2009). Hubinka et al. (2011) shows first results from the rig behavior.

Test Setup

As already mentioned the investigated test setup consists of a single stage unshrouded transonic HPT turbine, an S-shaped turning mid turbine frame followed by a shrouded counter-rotating LP turbine. For the EU project DREAM two TMTF configurations were designed. The basic configuration was done by MTU Aero Engines with an length to height ratio of about 3.5 (h_{inlet}/l, see Figure 1) and the second design was developed by Volvo Aero which is 10% shorter with endwall contouring applied at the hub to avoid additional losses and generate the same inflow conditions for the LP-turbine as the baseline configuration. To ease manufacturing and reduce the costs both TMTF setups were designed without fillets. In this paper the basic configuration will be discussed. Figure 1 represents a meridional section of the test facility with this TMTF design. The incoming air is accelerated by the HP vanes in circumferential direction and impinges on the HP rotor designed with a cylindrical outer contour. Then it is turned by the struts of the TMTF in

negative direction relative to the rotation of the HP rotor and the air enters the counter-rotating LP turbine assembled at a larger diameter. Further downstream the flow leaves the test setup through the straight supporting struts of the front bearing shield and the downstream diffuser.
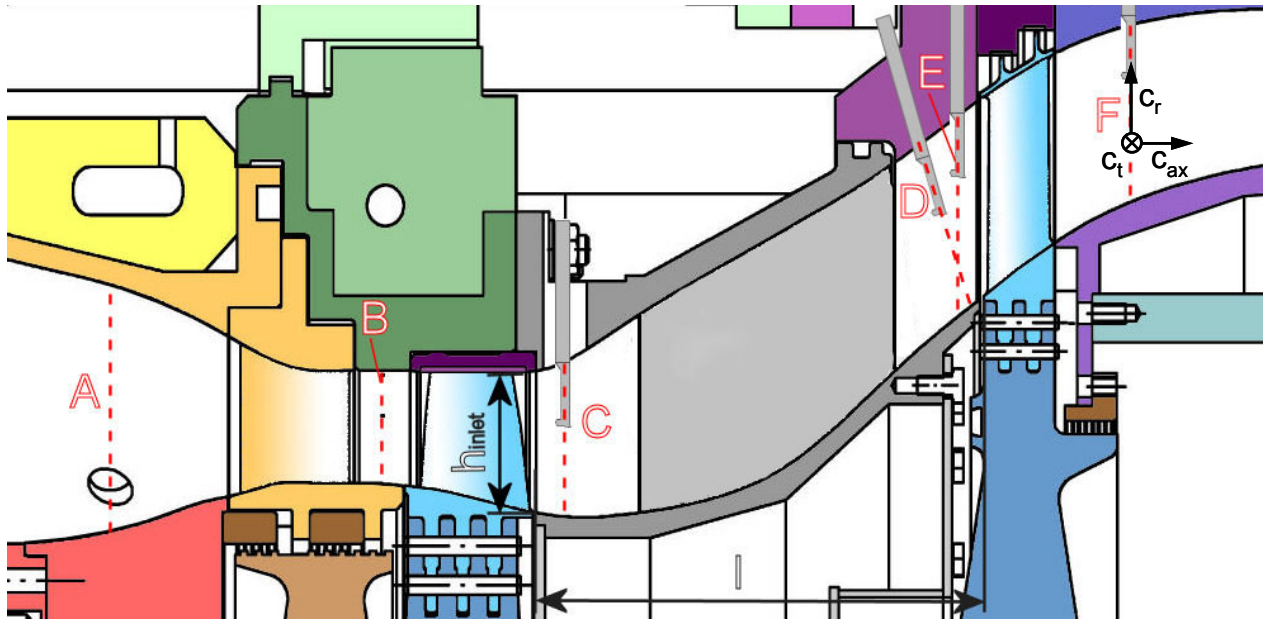

Figure 1 Meridional section of the test setup with probe measurement planes (C, D, E, F)

Design Intent TMTF

Turning strut or TMTF designs feature low aspect ratios around 0.5, with boundary layers on hub and casing as well as on the vane surfaces to be highly 3D in state. Little is known about transition mechanism at this highly turbulent and unsteady flow. In addition leading edge diameter and chord length for a TMTF is about one order in magnitude larger than for a standard LPT vane and the precise prediction of vortical structures and secondary flows becomes critically important.

Objective for the baseline design was to investigate the flow in a TMTF type first LPT stage with engine like inlet condition, i.e. large wakes and the strong turbulence structures generated by the complex shock system of the transonic HPT. From the rig data governing flow mechanisms will be elaborated. Furthermore, the baseline configuration is designed close to its loading limit using a three-dimensional design of the TMTF strut and keeping rotationally symmetric endwall contours (no endwall contouring). The struts have a maximum thickness to chord ratio of 22% to provide enough space for service lines like oil pipes and for load carrying. Close to separation careful code validation may be done to perform best design for future compact aero engines with TMTF architecture. For the design of the TMTF the MTU 3D multi-stage URANS solver TRACE (Vers. 6.2/ 6.3) together with the k-ω turbulence model was used in the steady mode.

Table 1 – Blading design parameters

Blading		HP vane	HP blade	TMTF	LP blade
vane/ blade no.	-	24	36	16	72
thickness/ chord ratio	-	0.31	0.19	0.22	0.12
aspect ratio H/l_{ax}	-	1.15	1.37	0.53	2.94
rel tip gap s/H	%H	-	unshrouded	-	shrouded
Reynolds Re 10^{-6}	-	2.38	1.1	1.86	0.46
		HPT			
work parameter DH/c_t^2	-	-1.624			
flow parameter c_{ax}/c_t	-	0.531			
Degree of reaction	-	0.338			

4

Table 1 displays the main blading design parameters for the HPT stage and the TMTF. The HP turbine consists of 24 choked vanes and 36 blades. For the LP stage a blade count of 16 struts and 72 blades was chosen in order to minimize the risk of excitation of the LP turbine as well as to have a periodicity between the HP vanes and the turning struts of 45 deg (two strut pitches). To ease unsteady CFD calculations the number of blades was chosen to have a periodicity of the rig consisting of the HPT, the TMTF and the LPT of 90 deg.

The HP vanes as well as the outer casing downstream the TMTF struts are fully rotatable in circumferential direction. This enables area traverses for probe and rake measurements. To gain a detailed understanding of the flow field upstream and downstream the TMTF and also downstream the LP turbine five-hole-probe (FHP) measurements in four planes were performed, see Figure 1 (plane C, D, E and F).

Instrumentation and measurement locations

Full area traverses with five-hole-probes (IST, RWTH Aachen) were performed in the plane downstream the HPT stage (plane C) over one HP vane pitch (15 deg) and over two strut pitches (45 deg) downstream the TMTF (D, E), respectively, to gain the full periodicity between the non-rotating blades. The radial measurement positions were realized by a traverse gear to rotate the probe and move it in- and outwards. To be able to perform full area traverses the HP vanes (plane C) and the probe (plane D, E, F), respectively, are mounted in circumferentially fully rotatable gear rings. Due to the strong slope of the duct downstream the turning struts a probe with an inclined head of 115 deg relative to the probe shaft axis was applied.

The measurement systems includes 15 multi channel pressure transducers PSI 9016 with a total amount of 240 channels and an accuracy of 0.05 % full scale and four National Instruments Field Point FP-TC-120 eight-channel thermocouple input modules and one FP-RTD-122 resistance thermometer input module. Table 2 shows the measurement uncertainties of the five- hole-probe measurements. These values contain the error due to the approximation and the systematic error of the PSI Modules. The measurement uncertainties of the static pressure taps are +/- 1 mbar.

Table 2 – Measurement uncertainties for the Five-Hole probe measurements

Mach number Ma	[-]	0.005	-0.004
Yaw angle α	[deg]	0.3	-0.3
Pitch angle γ	[deg]	0.5	-0.4
Total pressure p_t	[mbar]	3	-3
Static pressure p	[mbar]	5.4	-5.1
Total temperature T_t	[K]	0.6	-0.5
Static temperature T	[K]	0.7	-0.8

OPERATING CONDITIONS

Table 3 displays the main parameters of the operating point. The investigated aero design has an overall pressure ratio of 4 at design point. The total pressure ratio is 3 for the HPT and 1.3 for the LPT. The HP vanes are operating under choked conditions; therefore the reduced mass flow is constant for all investigated conditions. The Mach number at TMTF inlet at design point with a value of about 0.5 is representative for realistic duct inlet conditions of modern jet engines with a single stage HPT at cruise operating point.

Table 3 – Operating conditions for the aero design point

		HPT	LPT
reduced speed	rpm/sqrt(K)	524.4	195.3
inlet reduced mass flow	kg·sqrt(K)/s/bar	81.2	214.6
stage total pressure ratio	-	3	1.3
power	kW	1710	340

RESULTS AND DISCUSSION

Duct Inlet Flow

The flow leaving the HP turbine is highly three-dimensional with strong secondary flows, wakes and also shocks. These features have to be taken into account when designing a downstream component, especially a turning wide chord vane in an S-shaped duct. Figure 2 shows the circumferentially averaged distribution for yaw and pitch angle, Mach number as well as static and total pressure over the relative channel height. The arrows on the abscissa in the diagrams indicate the unit of axis scale of the corresponding flow parameter. The definition of the positive yaw angle is in the direction of rotation of the HPT for all planes (also downstream the LPT, plane F).

Figure 2 – Circumferentially Averaged Five-Hole-Probe results downstream the HP stage (plane C)

The static pressure distribution depicted in Figure 2d shows the typical positive pressure gradient from hub to casing of an annular duct increased by the presence of the first bend of the duct. Figure 2a displays the yaw angle distribution where a maximum variation over the channel height of 42 deg can be seen which requires a 3D design of the following TMTF strut. Due to the tip gap of the shroudless HPT less energy is extracted close to the casing. This leads to an unloading of the rotor and therefore the flow is less turned. The total pressure increases due to this fact as well (Figure 2e). The Mach number distribution in Figure 2c is strongly changing over the height with a maximum difference of 0.24. Two lower Mach number regions can be clearly identified which are the results of the lower passage vortex (LPV) and the tip leakage vortex together with the upper passage vortex (UPV), respectively. These structures can also be seen in the yaw angle and total pressure distribution (see Figure 2a and 2e) whereas the upper minimum corresponds to the UPV and the tip leakage vortex and the lower one is a result of the LPV. This highly unsteady inlet flow challenges the following TMTF to provide the LP turbine with adequate flow conditions.

Flow Through the TMTF Passage

Figure 3 and Figure 4 give the static pressure distribution by means of the pressure recovery coefficient C_p along the TMTF endwalls and the turning struts, respectively. C_p is defined as followed:

$$C_p = (p_n - p_C)/(p_{tC} - p_C) \qquad (1)$$

p_n represents the pressure at position n and p_{tC} and p_C are the total and static pressure in plane C. Figure 3 shows the static pressure distribution along the TMTF hub endwall on the left (a) and the casing endwall on the right (b) over one strut pitch. The black dashed lines indicate the position of the strut leading and trailing edge, respectively. In Figure 3a the black arrow on the left side indicates the unit of axis scale of C_p of 0.5. This value is also valid for Figure 3b.

At TMTF inlet the static pressure is very homogenous over the circumference at the hub contour, see Figure 3a. Further downstream the pressure diverges due to the potential field of the strut leading edge and the influence of the duct curvature. In contrast to an S-shaped duct without struts where the pressure increases due to the first bend of the duct (see Marn et al. 2007 and Marn et al. 2009a) the pressure is constant due the aero design of the duct and the blockage effect and the aft-loaded design of the strut. This can be nicely seen at about 50% of the strut passage (red line) at the hub and on the casing (Figure 3b) as well. The blockage effect of the leading edge (first dashed line) is indicated by a steep pressure drop. Within the strut passage the usual pressure gradient from suction to pressure side can be nicely seen. Starting from about 60 % of the axial strut chord length the flow is again accelerated due to the turning of the struts.

Figure 3a also shows that although the pressure still varies at strut exit it becomes quite homogenous before entering LPT. This effect is also present at the casing where the static pressure is even more uniform at LPT inlet, see Figure 3b. In contrast to the hub endwall a strong pressure rise at duct inlet due to the first duct curvature can be detected at the casing. Whereas the pressure drop due to the acceleration around the strut leading edge appears similar to the pressure distribution at the hub. Moving further downstream the static pressure is quite stable until 30 % chord length until it starts to rise on the PS and decreases on the SS. Similar to the flow at the hub endwall the flow accelerates along the full channel width at about 70 % of the strut chord length but the pressure drop is not that pronounced due to the longer chord length of the strut at the casing compared to the hub and also the curvature of the strut is much smoother in this area.
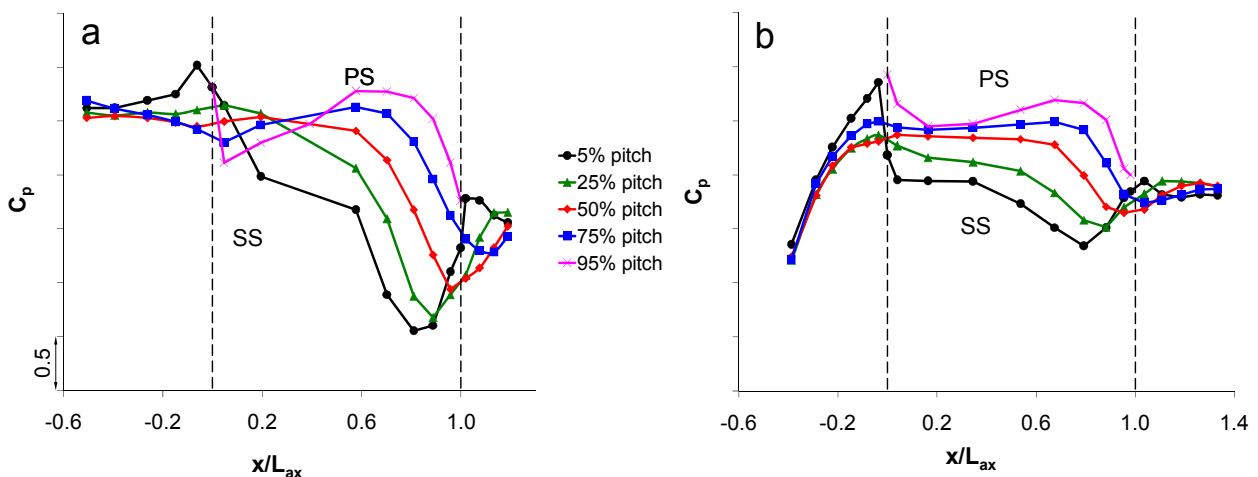

Figure 3 - Static pressure distribution along the TMTF hub (a) and casing (b); the arrow on the left side of the diagram indicates the unit of axis scale for C_p
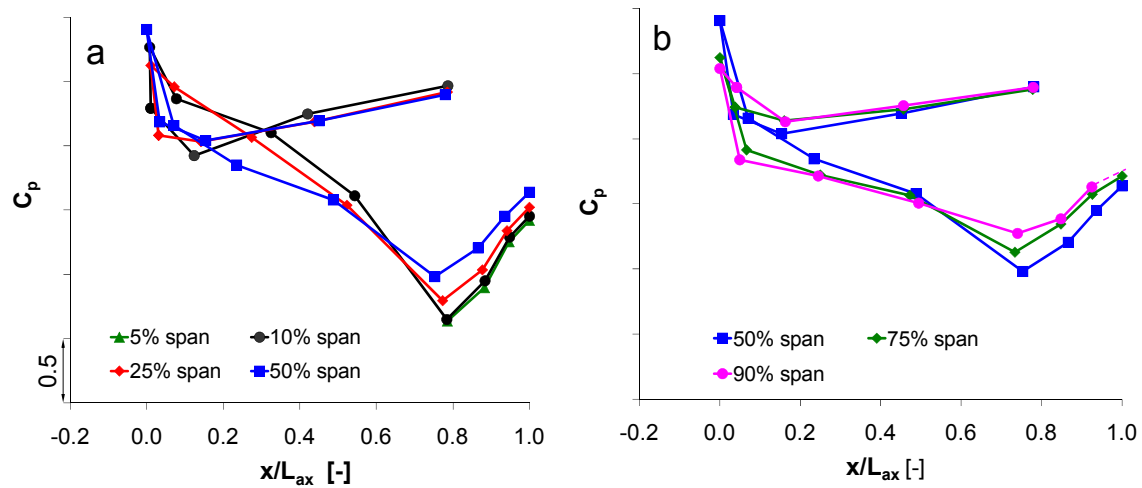
Figure 4 – Static pressure distribution along the turning strut over 5 different channel heights, from 5 to 50 % span (a) and from 50 to 90 % span (b)

The turning strut was instrumented with static pressure taps to acquire the static pressure distribution at five different channel heights (5, 10, 25, 50, 75 and 90 % span). The results of these measurements are presented in Figure 4. The left diagram (Figure 4a) includes the static pressure distribution form 5 to 50 % span and the right one (Figure 4b) shows the results from 50 to 90 % span along the axial chord length of the strut. In the left diagram (Figure 4a) the black arrow again represents the unit of axis scale of the pressure distribution similar to Figure 3. In Figure 4b the last point of the static pressure distribution on the SS at 90% span had to be replaced by a mean value between 75% span and the pressure at the casing because at this position the pressure tap did not deliver a proper value. The mean value is indicated by the dashed magenta line.

The static pressure taps at 5 % span were only applied at the rear part of the strut SS to detect a possible corner separation which was expected from CFD predictions but from the pressure distribution this could not be identified. However, the oil flow visualization (Figure 5) showed the evidence of a separation. This will be discussed later on.

From the pressure distributions in Figure 4 the change of the incidence angle over the channel height can be observed. Due to the yaw angle distribution shown in Figure 2a the incidence angle is strongly negative in the lower part of the flow channel up to 50% span and becomes even positive close to the casing where the tip leakage flow is present. The peak suction on the SS occurs at about 75% of the axial chord length. This is an effect of the aft loaded design of the strut. This leads to lower losses compared to a front loaded design due to the fact that secondary flow effects like the passage vortices are generated further downstream compared to a front loaded design. The influence of the diffusing S-shaped duct can be nicely seen in the pressure rise at the strut PS.

For a better understanding of the flow through the turning mid turbine frame and to identify if there is a separation at the strut suction side - hub corner oil visualization has been applied at the strut SS and the hub endwall. The blades and the endwalls of the TMTF were painted in pink and white, respectively, to ease the identification of the origin of shear stress lines. Figure 5 shows the results gained from these investigations. Up to about 40% channel height the flow along the strut SS seems to follow the slope of the duct quite well. In contrast to former publications with wide chord vanes (e.g. Pullan et al. (2003), Pullan et al. and (2005) Marn et. al. (2009a)) the lower passage vortex is to weak to push the fluid from the hub endwall onto the strut SS towards midspan (Figure 5a). This seems to be a result of the aft-loaded and three-dimensional design of the blade. Nevertheless the influence of the cross passage pressure gradient can be seen very well on the hub contour, see Figure 5b. Close to the casing the flow is pushed away from the casing endwall down the strut SS which indicates the presence of an upper passage vortex. On the strut suction side close to the hub a small separation is present, see red dashed circle in Figure5. It is important to know that

the design intend was to have a vane profile which is close to separation in this region to see if the CFD calculations can predict this phenomenon in the right way. Figure 6 displays a comparison of the oil flow visualization with a post-test CFD result where it can be nicely seen that the streamlines in this region as well as the small separation have been predicted quite well. It is assumed that the corner separation is mainly a result of the corner flow with two boundary layers between the hub contour and the strut. If a fillet would exist like in a real engine the separation could probably be avoided. A further step to enhance the flow in this region would be to introduce non-axisymmetric endwall contouring at the hub like it was done for the second TMTF setup designed by Volvo Aero.
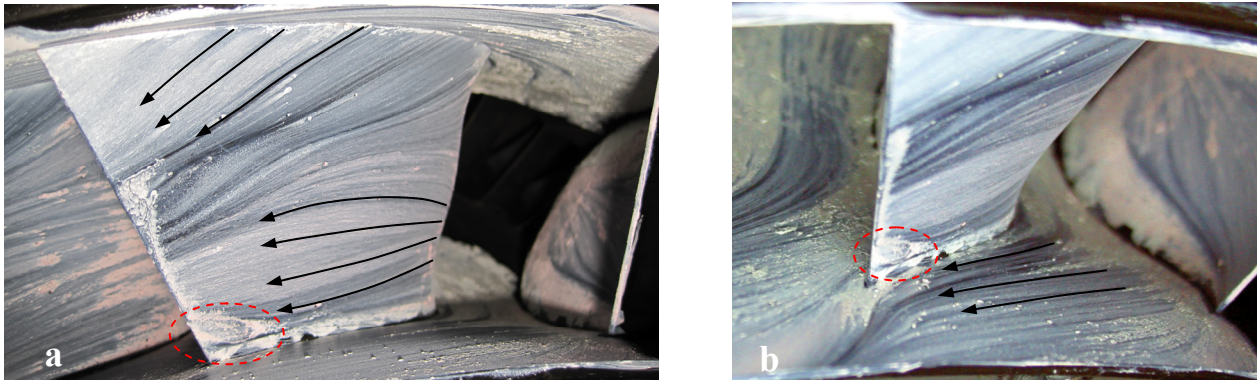

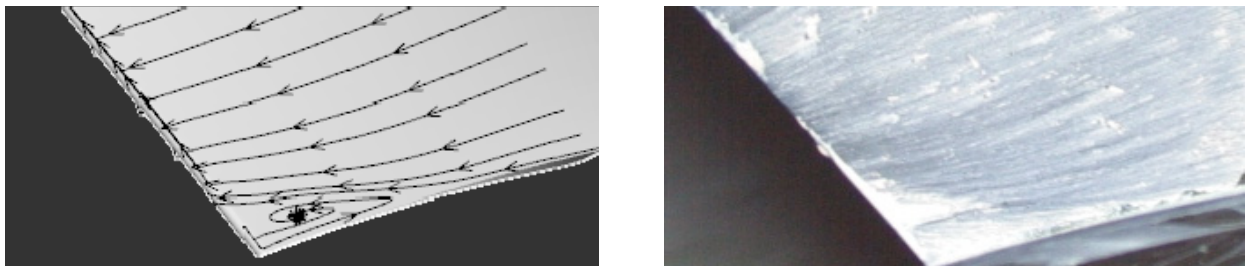**Figure 5 – Oil flow visualization of the TMTF at the strut SS (a) and on the hub endwall (b) viewed from downstream**

Figure 6 – Oil flow visualization of the TMTF at the strut SS (a) compared to CFD post-test streamlines (b)

TMTF exit flow

In Figure 7 the circumferentially averaged distribution of yaw and pitch angle, Mach number, static and total pressure are depicted for both planes downstream the turning strut. Figure 1 and the sketch of the flowpath in Figure 7 show the position of these planes. Compared to the circumferentially averaged distributions at the TMTF inlet all flow parameters are much more homogenous over the channel height which indicates that most of the secondary effects emanating from the HP rotor are mixed out while the flow passes the TMTF. The difference between the mean yaw angle in plane C compared to the one downstream the strut (plane D and E) is about -45 deg (positive in direction of HP rotor rotation). This means that the turning of the flow is stronger than the geometrical turning of the strut (~40 deg). Close to the casing (from plane D to E) and also close to the hub (from plane E to D) the yaw angle increases which could be the influence of the downstream LPT rotor which accelerates the flow. The lower Mach number and total pressure close to the hub indicate the presence of a thick boundary layer (BL). Further downstream in plane D the large BL close to the hub cannot be detected anymore due to the influence of the downstream LPT like it has been found in the yaw angle distribution.

In Figure 8 the contour plots of the Mach number for plane D (a) and plane E (b) are given. As mentioned before the measurements were performed over two strut pitches (45 deg) to gain the full periodicity between the HP stator and the strut (3 HP vanes over 2 struts). The results revealed a small influence of the effects resulting from the relative positions of the HP vane trailing edge to the

strut leading edge but the main occurring secondary flow phenomena are similar in both flow channels. Therefore, the contour plots of the Mach number in Figure 8 are depicted only over one pitch for both planes downstream the turning strut. Blue areas represent a low and red areas a high Mach number level. The black dashed line indicates the wake emanating from the strut whereas the black arrows indicate the rotational direction of the occurring vortical structures gained from yaw and pitch angle distribution as well as the vorticity. One main dominating vortical structure can be identified which extends nearly over the full cross sectional area. It is assumed that this is the remains of the HP rotor tip leakage vortex and lower passage vortex. They mix out on their way through the TMTF but their vorticity diffuses across the passage and result in this rotating feature. In the upper left close to the suction side (SS) the upper passage vortex can be identified which was already detected in the oil flow visualization. Furthermore, close to the casing a third vortical structure is visible which seems to be the result of the small appearing separation on the strut SS. It is assumed that this is a result of the suction surface hub corner operating at its loading limit. Moving from plane D to E the skewing of the wake due to the swirl can be detected at the upper part of the contour plot in Figure 8a where the plane is further downstream relative to plane D, see Figure 1. The upper passage vortex has been partly merged with the wake of the strut which is indicated through the smaller area of low Mach number.
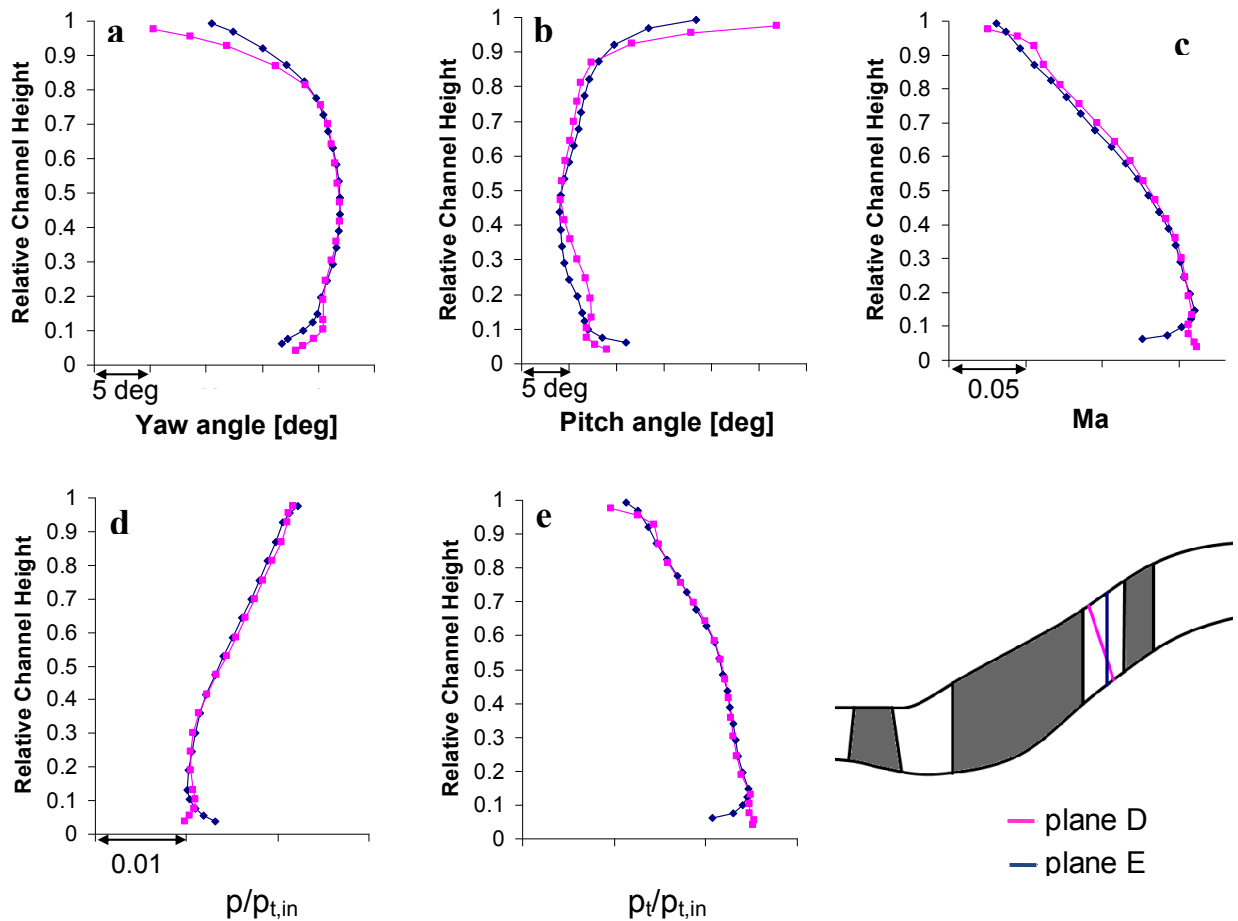

Figure 7 – Circumferentially Averaged Five-Hole-Probe results downstream the turning strut (plane D and E)
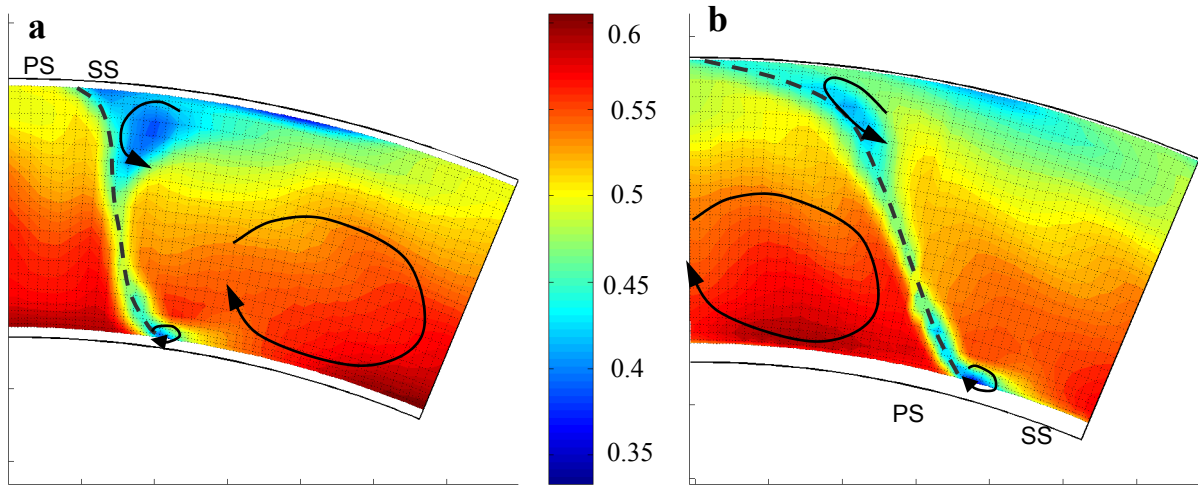
Figure 8 – Mach number distribution downstream the turning strut in plane D (a) and plane E (b), respectively, with rotational direction of vortical structures (black arrows); viewing direction from downstream
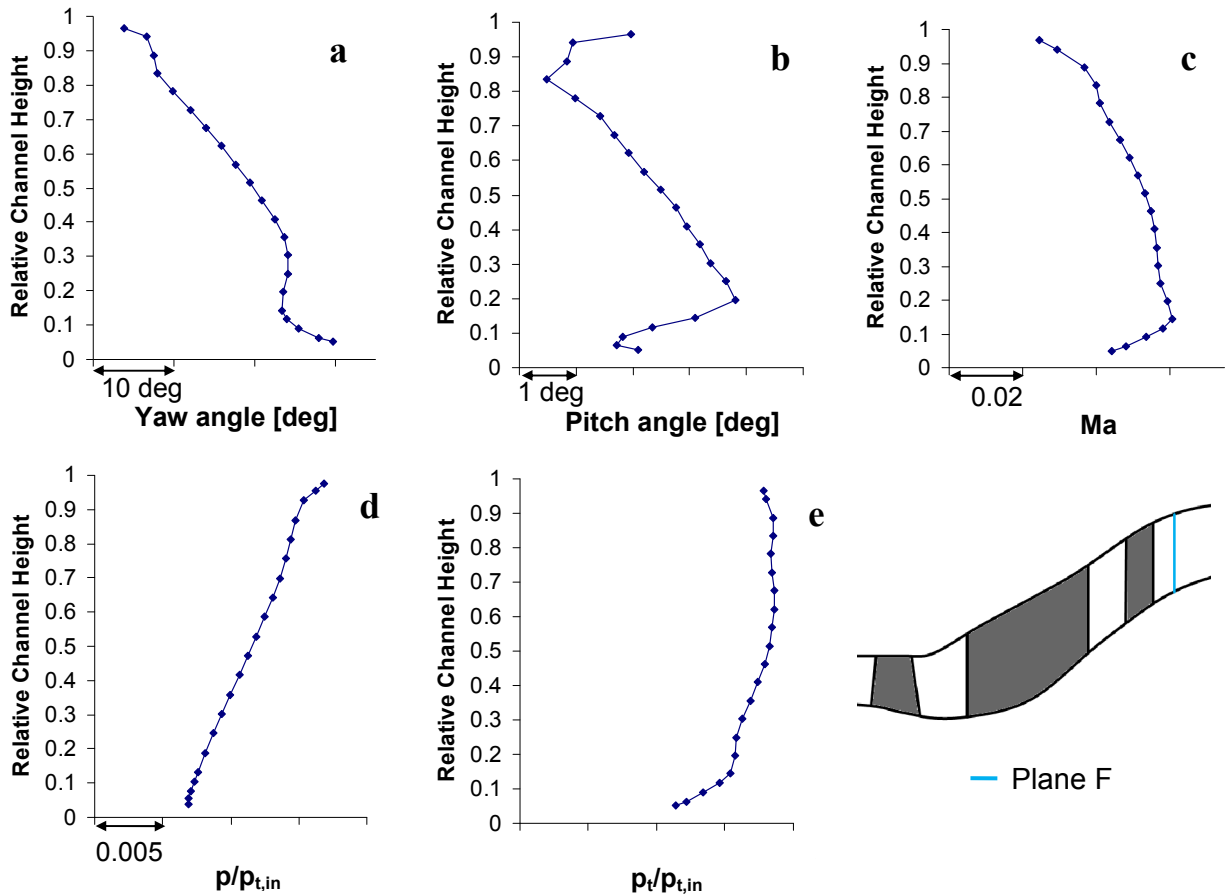

Figure 9 – Circumferentially Averaged Five-Hole-Probe results downstream the LP stage (plane F)

Results downstream LP rotor

In Figure 9 the circumferentially averaged distributions in plane F downstream the LPT are presented. The positive yaw angle is defined like in the other planes in direction of rotation of the HPT. The diagrams show the typical distribution downstream a shrouded LPT. One main difference to an unshrouded turbine is that there is no high tip leakage flow which would lead to a high Mach number region, compare Figure 2c and Figure 9c. Due to the missing usually following next LP

stage the blade had to be designed different to an engine-realistic LPT. The radius at the hub was increased to reduce the swirl as well as the static pressure and further reduce the risk of separation in this region. Although the flow does not separate on the hub a large boundary layer is present which can be seen in the Mach number distribution (Figure 9c) as well as the total pressure distribution (Figure 9e). The gradient in the static pressure distribution shown in Figure 9d is mainly a result of the second bend of the flow channel.

CONCLUSIONS

The flow through a turning mid turbine frame (TMTF) and its interactions with an upstream transonic HP turbine and a counter-rotating LP turbine downstream the duct has been investigated. The main objective was to get a better understanding how the secondary flows, shocks and wakes emanating from the HPT influence the flow through the TMTF. Due to the low number of vanes (16), the low aspect ratio and the comparatively high turning of the flow secondary flows were found downstream the strut but due to the aft-loaded and 3D design of the TMTF strut they were found not very pronounced for such a configuration. The five-hole-probe (FHP) results revealed that secondary flows like the lower and upper passage vortex as well as the tip leakage vortex coming from the HP turbine are mostly mixed out after they passed the turning strut but result in a large but weak vortical structure which reaches nearly over the whole cross section. This produces strong circumferential and radial gradients. Nevertheless the downstream situated shrouded LP rotor especially designed for this configuration could handle this flow and operated stable.

Further investigations will focus on the influence of the unsteady flow features emanating from the HPT. Their impact on the TMTF flow will be investigated by means of fast response pressure sensors and FRAP probes. In a further step a second TMTF design from Volvo will be investigated. This TMTF will be 10 % shorter than the baseline configuration with non-axisymmetric endwall contouring applied at the hub.

REFERENCES

Arroyo Osso C., Wallin F., Johansson G., (2008), "Experimental and Numerical Investigation of an Aggressive Intermediate turbine duct - Part 2: Flowfield under Off-design Inlet Conditions", 26th AIAA Applied Aerodynamics Conference, AIAA-2008-7055.

Erhard J., Gehrer A., (2000), "Design and Construction of a Transonic Test Turbine Facility", ASME Paper 2000-GT-480.

Harvey N. W., Brennan G., Newman D. A., Rose M. G., (2002), "Improving Turbine Efficiency Using Non-Axisymmetric End Walls: Validation in the Mult-Row Environment and with Low Aspect Ratio Blading", ASME-paper GT-2002-30337.

Hubinka, J., Santner C., Paradiso B., Malzacher F., Göttlich E., Heitmeir F., (2009), „Design and Construction of a Two Shaft Test Turbine for Investigation of Mid Turbine Frame Flows", ISABE Paper ISABE-2009-1293.

Hubinka, J., Paradiso B., Santner C., Göttlich E., Heitmeir F., (2011), "Design and Operation of a Two Spool High Pressure Test Turbine Facility", submitted for 9th European Conference of Turbomachinery Fluid Dynamics and Thermodynamics.

Lavagnoli S., Yasa T., Paniagua G., Duni S., Castillon L., (2010), "Aerodynamic Analysis of an Innovative Low Pressure Vane Placed in a S-Shape Duct", ASME paper GT2010-22546.

Marn, A., Göttlich, E., Pecnik, R., Malzacher, F. J., Schennach, O., Pirker, H. P., (2007), "The Influence of Blade Tip Gap Variation on the Flow through an Aggressive S-Shaped Intermediate Turbine Duct Downstream a Transonic Turbine Stage - Part I, Time-Average Results," ASME Paper GT2007-27405.

Marn A., Göttlich E., Leitgeb T., Heitmeir F., (2009a), "Shorten the Intermediate Turbine Duct Length by Applying an Integrated Concept", Journal of Turbomachinery Vol. 131, Issue 4.

Marn, A., Göttlich, E., Malzacher, F., Heitmeir, F., (2009b), "Comparison Between the Flow Through an Aggressive and a Super-Aggressive Intermediate Turbine Duct," submitted for 19th International Symposium on Air Breathing Engines, Montreal, Canada.

Miller R.J., Moss R.W., Ainsworth R.W., Harvey N.W., (2004), "The Effect of an Upstream Turbine on a Low-Aspect Ratio vane", ASME Turbo Expo, GT2004-54017.

Neumayer F., Kulhanek G., Pirker H.P., Jericha H., Seyr A., Sanz W., (2001), "Operational Behaviour of a Complex Transonic Test Turbine Facility", ASME Paper 2001-GT-489.

Norris G., Dominy R. G., Smith A. D., (1999), "Flow Instabilities Within a Diffusing Annular S-Shaped Duct", ASME Paper 99-GT-70.

Pullan, G, Denton, J., Dunkley M., (2003), "An Experimental and Computational Study of the Formation of a Streamwise Shed Vortex in a Turbine Stage", Journal of Turbomachinery, Vol. 125, pp. 291-297.

Pullan, G., Denton, J., Curtis E., (2005), "Improving the Performance of a Turbine with Low Aspect Ratio Stators by Aft-Loading

Wallin F., Arroyo Osso C., Johansson G., (2008), "Experimental and Numerical Investigation of an Aggressive Intermediate Turbine Duct: Part 1 - Flowfield at Design Inlet Conditions", 26th AIAA Applied Aerodynamics Conference, AIAA-2008-7056.